Axial Thermal Rotation of Slender Rods

Dichuan Li, Nikta Fakhri, Matteo Pasquali, and Sibani Lisa Biswal*

Department of Chemical and Biomolecular Engineering, Rice University, Houston, Texas 77005, USA

(Received 19 January 2011; published 3 May 2011)

Axial rotational diffusion of rodlike polymers is important in processes such as microtubule filament sliding and flagella beating. By imaging the motion of small kinks along the backbone of chains of DNA-linked colloids, we produce a direct and systematic measurement of axial rotational diffusivity of rods both in bulk solution and near a wall. The measured diffusivities decrease linearly with the chain length, irrespective of the distance from a wall, in agreement with slender-body hydrodynamics theory. Moreover, the presence of small kinks does not affect the chain's axial diffusivity. Our system and measurements provide insights into fundamental axial diffusion processes of slender objects, which encompass a wide range of entities including biological filaments and linear polymer chains.

DOI: 10.1103/PhysRevLett.106.188302 PACS numbers: 82.70.Dd, 05.40.Jc, 82.70.Kj

Unlike spheres, highly anisotropic objects diffuse in a complex manner, particularly so if they are flexible. The combined effects of shape anisotropy, internal degrees of freedom, and environment greatly influence their behavior. Some of these dynamical effects are now being understood, like the strong coupling between translational diffusion and transverse rotation (usually simply termed rotation) [1] and enhanced transverse rotational diffusion of slightly flexible rods in crowded environments [2]. Despite its crucial importance in structuring of liquid crystals [3] and in biological processes such as lipid bilayer dynamics [4] and microtubule sliding [5,6], rotational diffusion around the long axis (axial rotation) of rodlike molecules is still poorly characterized and not understood. Direct measurement of axial rotation is challenging because most of the electro-optical properties of cylindrical macromolecules are also axisymmetric [7]. NMR relaxation [4], fluorescence anisotropy decay [8], and 3D tracking [6,9] have been used to measure the axial rotation of rodlike molecules. The first two techniques measure ensemble average properties and are model-dependent; the third lacks sufficient accuracy to capture diffusion.

Rodlike colloidal model systems [8–10] can be visualized accurately in real time and space and have tunable length and stiffness. Their axial symmetry can be broken simply, as shown by the recent observation of the axial rotation of a rodlike tetramer along its long axis [10]. Here, we report a systematic study of axial rotational diffusivity of slender rods by directly observing with high accuracy the dynamics of asymmetric DNA-linked magnetic colloidal particles.

Axial rotational diffusion of elongated colloids was reported in 1827 by Robert Brown in the first report on thermal (now called Brownian) motion: ''oval particles ... their motion consisting in turning usually on their longer axis, and then often appearing to be flattened'' [11]. Brown's observation relied on the slight asymmetry of arsenic trioxide flakes. The same symmetry breaking principle is used in our experiments, but the measurements are quantitative with high precision. The colloidal rods consist of DNA-grafted paramagnetic particles aligned by a magnetic field and connected by linker DNA strands through hybridization [12,13]. Their axial rotation is revealed by the relative motions of small kinks along their backbones, recorded by video microscopy and analyzed by image processing. The kinks act as tracers and are sufficiently large for accurate imaging while small enough not to introduce significant deviation from a perfectly straight rod in terms of axial rotational diffusivity. We first track the motion of kinks in 6–54 μm stiff rigid rods undergoing Brownian motion near a flat substrate to measure their axial rotational diffusivities. Subsequently, we apply a magnetic field to control the distance between the rods and the substrate and measure their axial rotational diffusivities in bulk. These measured diffusivities match reasonably well with theoretical predictions [7,14–16], confirming the validity of the slender-body hydrodynamic theory.

These rigid rods are made by linking 15-base oligonucleotides-grafted [13,17] (surface density 5×10^4 strand/μm^2) paramagnetic polystyrene MyOne beads (Dynal Biotech, Oslo, Norway) under a uniform magnetic field [13]. Because of slight nonuniformity in the distribution of magnetic material inside the particles, their centers of mass deviate from the straight-line magnetic dipole alignment, forming kinks. These kinks are permanently set by hybridization of linker DNA and particle surface DNA. When the field is removed, the linked chains undergo quasi-2D Brownian motion near the substrate due to confinement by gravity [Figs. 1(a)–1(h) and 2(a)]. To quantify the stiffness of these chains with contour length L, their persistence length Lp is measured to be 50 ± 7 mm (L/Lp ranging from 5×10^{-5} to 10^{-3}) via Fourier mode analysis of their curvature induced by thermal fluctuations [13]. The Brownian motion of the isolated chains is recorded and the axial rotational angle

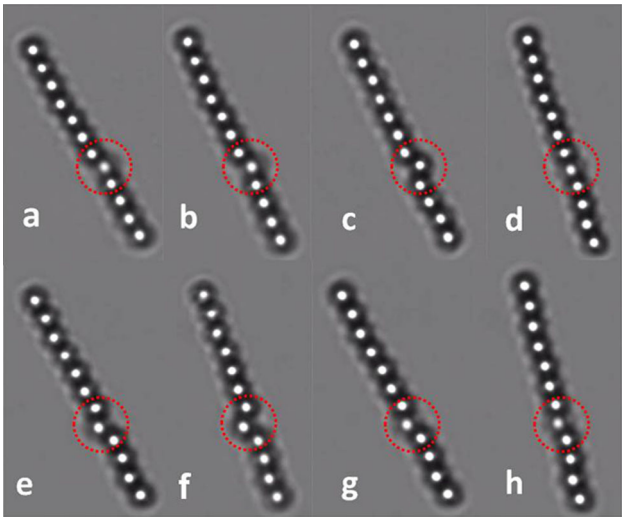

FIG. 1 (color online). Snapshots of a 12-bead rigid DNA-linked chain under Brownian motion in aqueous solution near the bottom substrate. The snapshots (a)–(h) are taken 10 seconds apart, and the red dashed circles are highlighting the kink formed by the 7th, 8th, and 9th beads from the left. The unusual large size ($\phi \approx 75°$) of this kink is only for demonstration, whereas the kinks used to measure the axial rotational diffusivities in this Letter are much smaller than this ($14° \leq \phi \leq 25°$).

$\Phi(s_i)$ is analyzed along the chain's arclength s for each bond angle i (see [18] for details).

For each chain near the substrate (Fig. 4, bottom-left inset), we measure the transverse rotational diffusivity and compare that with theory [1] to confirm that it is not attached to the substrate (Fig. S1 in [18]). To measure bulk axial rotational diffusivity, we use a magnetic gradient field to levitate the rod to ~ 10 μm above the substrate. The chain diffuses freely along the vertical axis, indicating that vertical forces are balanced (Fig. 4, top-right inset).

The distribution of bond angles between each pair of bond vectors (bond number) can be measured [Fig. 3(a)]. For example, the bond angle between the 1st and 2nd vectors (bond number 1) ranges from $-5°$ to $+5°$, while the bond angles between the 7th and 8th vectors (bond number 7) range from $-15°$ to $+15°$. Since this range of angles is symmetric about 0°, it indicates that the chain is making full axial rotations. We can calculate $\Phi(s_i)$ from the kinks whose bond angle exceeds 14° (chosen to minimize error while still providing a statistically sufficient number of kinks within a chain). For each kink, we compute $\Phi(s_i)$ based on the geometry [18] in Fig. 2(b), where solid lines represent a 3D construct and dashed lines are 2D projections on the image plane. The final calculated $\Phi(s_i)$ spans between 0 and π [Fig. 3(b)] and has a uniform distribution [Fig. 3(c)]. This indicates the rods undergo Brownian motion without any bias in the direction of axial rotation. Mean-squared displacement (MSD) of $\Phi(s_i)$ of each chosen kink within a rod is plotted against lag time Δt

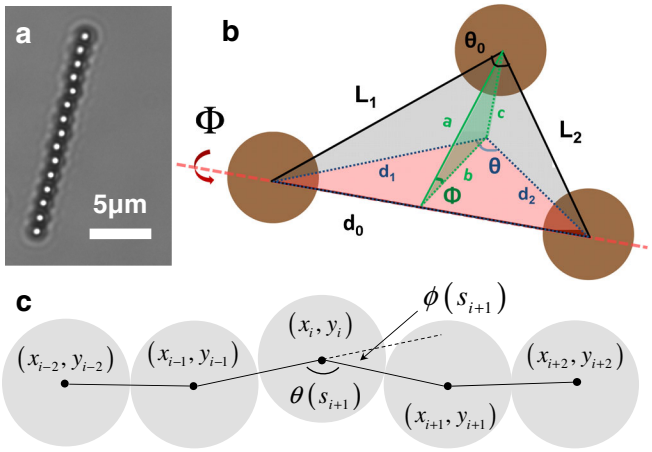

FIG. 2 (color online). Measuring axial rotation of a 15-bead DNA-linked chain by tracking motions of kinks. (a) Snapshot of a 15-bead DNA-linked chain undergoing Brownian motion. (b) Geometry of a kink in 3D configuration and its projection. (c) Definitions of position coordinates, bond angle $\phi(s_i)$, and tangent angle $\theta(s_i) = \pi - \phi(s_i)$ along the chain.

[Fig. 3(d)], i.e., the time elapsed between two measurements. Finally, the axial rotational diffusivities D_{ar} are calculated by fitting a straight line to the MSD vs lag time curve using the Einstein relation $\langle[\Phi(t + \Delta t) - \Phi(t)]^2\rangle_t = 2D_{\mathrm{ar}}\Delta t$. Measured diffusivities from different kinks within each rod are averaged to give the final values and standard deviations.

The drag coefficient of a rigid rod rotating around its long axis predicted by slender-body hydrodynamic theory [5,14,19] is approximately the sum of rotational drag coefficients of spheres, $8\pi\eta r^3$, constituting the rod, i.e.,

$$D_{\mathrm{ar}}^{\mathrm{Bulk}} = \frac{k_B T}{4\pi\eta r^2 L}, \tag{1}$$

where k_B is Boltzmann constant, T is the absolute temperature, η is the solvent viscosity, r is the bead radius, and L is the rod length.

To test the slender-body hydrodynamic theory, we measured the axial rotational diffusivities of rigid rods in bulk liquid. For each chain, a magnetic field is applied that has a gradient in the vertical direction but is uniform in the horizontal plane. The magnetic field in the horizontal plane induces dipole interactions that keep the chain from rotating in the image plane [17,19] but does not affect the force balance in the image plane; therefore, the axial rotational diffusion of the chain should not be affected. The measured bulk axial rotational diffusivities of the 6 rigid chains (green circles in Fig. 4) decrease with increasing chain length in agreement with slender-body hydrodynamic theory (red line in Fig. 4).

Near a wall, diffusion is slower due to the hydrodynamic reflections of the rod on the wall, according to [15,20]

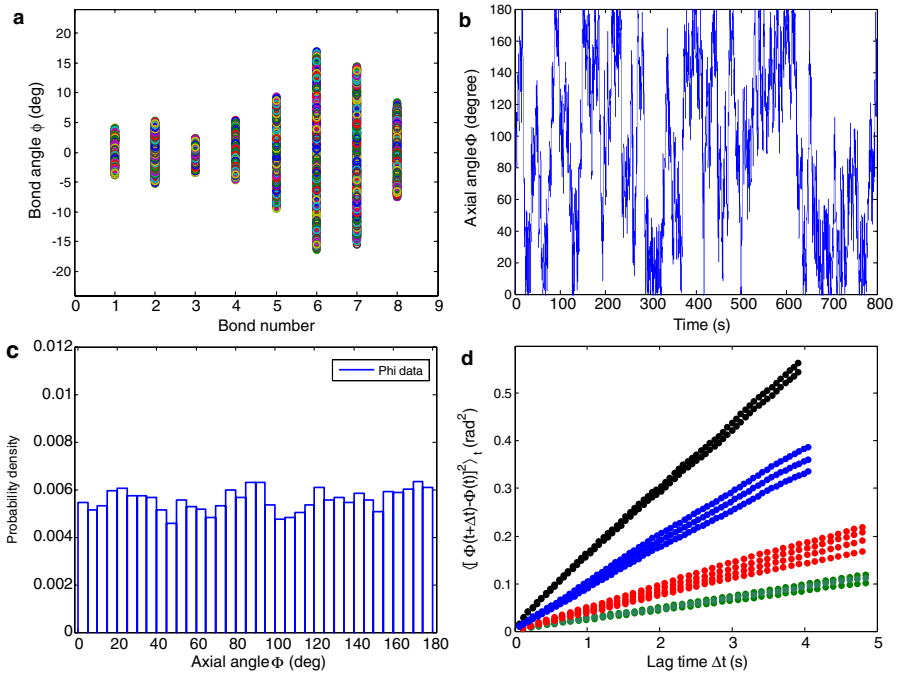

FIG. 3 (color online). (a) Overlay of bond angles ϕ of all kinks in a 10-bead chain within 800 seconds. (b) Axial rotational angle $\Phi(t)$ measured from the sixth kink of the same chain in (a). (c) Histogram of the same angles in (b). (d) Typical plot of axial rotational angular MSD as a function lag time of 10-bead (black circle), 16-bead (blue circles), 30-bead (red circles), and 40-bead (green circles) chains in bulk.

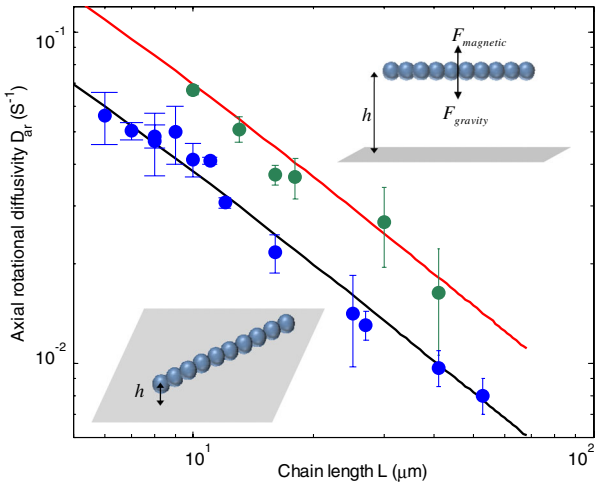

FIG. 4 (color online). Axial rotational diffusivities of rigid rods. Slender-body hydrodynamics theory predictions of axial rotational diffusivities in bulk (red line) and near a wall (black line) as a function of rod lengths. Experimental measured axial rotational diffusivities of rods in bulk (green circles) and near a wall (blue circles). Error bars are standard deviations of axial rotational diffusivities obtained from different kinks of the same chains. (Insets) Schematic illustrations of a chain near a wall (bottom left, where h is the distance between the center of the beads and the wall) and a chain elevated by a magnetic field (top right). Distances are not to scale.

$$D_{\mathrm{ar}}^{\mathrm{Wall}} = \frac{k_B T}{4\pi\eta r^2}\sqrt{1-(r/h)^2}, \tag{2}$$

where h is the distance between the center of the rod (beads) and the wall. We measure the axial rotational diffusivities of rigid rods near a wall by monitoring their Brownian motion near the glass substrate. Because of the high density of the paramagnetic beads ($\sim 1800\ \mathrm{kg/m^3}$), chains longer than 6 beads are confined in quasi-2D [13] and rarely fluctuate out of the focal plane (~ 300 nm). The data (blue circles in Fig. 4) fit reasonably well Eq. (2) with a power law of -1 (black line in Fig. 4) in a log-log plot. The right-hand side of Eq. (2) contains the same bulk diffusivity term as in Eq. (1) and a factor determined by the height of the rod above the substrate. Because no systematic deviation of data points from Eq. (2) is observed when using a single fitting parameter h ($h = r + 0.12\ \mu$m), all the chains, long and short, have approximately the same average height above the substrate. The value of the height is in agreement with both the height of the same chains calculated by using their short-axis rotational dynamics data [18] ($h = r + 0.13\ \mu$m, Fig. S1, see [18]) and the height of more flexible chains calculated from their bending relaxation dynamics ($h = r + 0.15\ \mu$m) [13]. The above evidence strongly suggests the validity of the previous hydrodynamic dissipation model.

To claim high precision in our axial rotational diffusivity measurement, we quantify all the major sources of error.

Error (1) comes from the inaccuracy in determining the particles' centers of mass positions. A ± 4 nm position error [17] would lead to a 1°–4° error in the $\Phi(s_i)$ measurement, depending on the instantaneous position of the kink. This random error source ultimately leads to a systematic underestimate of diffusivity by up to 3%. Error (2) comes from the fact that kinks are ubiquitous in any rod we measure. Depending on the size of each kink, its effect on the deviation of the axial rotational drag coefficient of the whole chain is given by the expression $\zeta^{\text{error}} = 6\pi\eta r z^2$ [21], where z is the particle center of mass deviation from the long axis. We use the theory for straight rigid rods that does not take into account the kinks with size $2° \leq \phi(s_i) \leq 20°$, which is equivalent to an overestimate of diffusivity by 2%. Error (3) results from the fact that the $\phi(s_i)$ angles should vary between $-\infty$ and $+\infty$ but are measured to be only between $-\pi/2$ and $\pi/2$. This effect is equivalent to confined 1D diffusion between 2 walls [22] and would saturate the MSD vs time curves [Fig. 3(d)] as time approaches the axial rotational relaxation time. This effect could potentially result in an underestimate of diffusivity by $O(t/2\pi^2\tau)$. We reduce this underestimation to less than 1% by limiting the time scale plotted to be less than 5% of the relaxation time scale. As seen in Fig. 3(d), the MSD vs time curves are straight within a 0–5 s time frame (relaxation time 200–1000 s). Error (4) is due to the assumption that both centers of mass of the particles [left and right in Fig. 2(b)] next to the kinked particle [top one in Fig. 2(b)] are on the rotation axis, which might not be true due to the fact that the kink arrangement within a rod is random and 3D in nature. Error (5) is caused by occasional tilting of the rods during recording that results in inaccurate particle distance measurement. Errors (4) and (5) are negligible (causing the error in the final measured diffusivity values to be $<1\%$) since the tilting angle and the degree of axial mismatch are small enough [17,23]. In summary, the upper bound of error is $\pm 3\%$, which is unprecedented in single rod axial rotational diffusivity measurements.

In this Letter, we have demonstrated a convenient and systematic approach to measure axial rotational diffusivities of colloidal rigid rods of length 6–54 μm, both in bulk and near a wall. We have shown that the experimentally measured diffusivities match reasonably well with slender-body hydrodynamics theory calculations. Our DNA-linked colloidal rods, with controllable length, rigidity, and elevation, in conjunction with the imaging and processing technique, provide an excellent prototype to study semiflexible filament axial rotation, twisting, and writhing dynamics. This opens the door to investigating polymer dynamics by using colloidal rods in both bulk and confined environments.

The authors gratefully thank George J. Hirasaki for insightful discussions. This work is supported in part by the Office of Naval Research YIP (Grant No. N00014-07-1-0820), the National Science Foundation (CBET-0955003), and the Welch Foundation (Grant No. C-1668).

*Corresponding author.
biswal@rice.edu.

[1] Y. Han *et al.*, Science **314**, 626 (2006).
[2] N. Fakhri *et al.*, Science **330**, 1804 (2010).
[3] J. Leisen *et al.*, J. Chem. Phys. **97**, 3749 (1992).
[4] R. W. Pastor, R. M. Venable, and M. Karplus, Proc. Natl. Acad. Sci. U.S.A. **88**, 892 (1991).
[5] J. Yajima and R. A. Cross, Nature Chem. Biol. **1**, 338 (2005).
[6] J. Yajima, K. Mizutani, and T. Nishizaka, Nat. Struct. Mol. Biol. **15**, 1119 (2008).
[7] J. G. Delatorre and V. A. Bloomfield, Q. Rev. Biophys. **14**, 81 (1981).
[8] R. L. Christensen, R. C. Drake, and D. Phillips, J. Phys. Chem. **90**, 5960 (1986).
[9] B. Nitzsche, F. Ruhnow, and S. Diez, Nature Nanotech. **3**, 552 (2008).
[10] L. Hong, S. M. Anthony, and S. Granick, Langmuir **22**, 7128 (2006).
[11] R. Brown, in *The Miscellaneous Botanical Works of Robert Brown*, edited by J. J. Bennett (Robert Hardwicke, London, 1866), Vol. 1, p. 487.
[12] D. C. Li, J. Rogers, and S. L. Biswal, Langmuir **25**, 8944 (2009).
[13] D. C. Li, S. Banon, and S. L. Biswal, Soft Matter **6**, 4197 (2010).
[14] R. G. Cox, J. Fluid Mech. **44**, 791 (1970).
[15] D. J. Jeffrey and Y. Onishi, Q. J. Mech. Appl. Math. **34**, 129 (1981).
[16] A. J. Hunt, F. Gittes, and J. Howard, Biophys. J. **67**, 766 (1994).
[17] D. C. Li, C. N. Lam, and S. L. Biswal, Soft Matter **6**, 239 (2010).
[18] See supplemental material at http://link.aps.org/supplemental/10.1103/PhysRevLett.106.188302 for materials and methods and a movie showing rotational diffusion of a 12-bead rodlike chain.
[19] S. L. Biswal and A. P. Gast, Phys. Rev. E **69**, 9 (2004).
[20] J. Howard, *Mechanics of Motor Proteins and the Cytoskeleton* (Sinauer Associates, Sunderland, MA, 2001).
[21] N. Suzuki *et al.*, Biophys. J. **70**, 401 (1996).
[22] T. Bickel, Physica (Amsterdam) **377A**, 24 (2007).
[23] J. C. Crocker and D. G. Grier, J. Colloid Interface Sci. **179**, 298 (1996).